Neurol Med Chir (Tokyo) 50, 756～764, 2010

Endoscopic Endonasal Pituitary and Skull Base Surgery

Naokatsu SAEKI, Kentaro HORIGUCHI, Hisayuki MURAI,
Yuzo HASEGAWA, Toyoyuki HANAZAWA*, and Yoshitaka OKAMOTO*

*Departments of Neurosurgery and *Otorhinolaryngology,*
Chiba University Graduate School of Medicine, Chiba

Abstract

Here we describe the procedures of endoscopic pituitary and skull base surgery in our institute. We also review the literature to reveal recent advances in this field. Endonasal approach via the sphenoid ostium was carried out for pituitary lesions without the nasal speculum. Postoperative nasal packing was basically not needed in such cases. For meningiomas, craniopharyngiomas, and giant pituitary adenomas, which required intra-dural procedures, nasal procedures such as middle nasal conchotomy and posterior ethmoidectomy, and skull base techniques such as optic canal decompression and removal of the planum sphenoidale were carried out to gain a wider operative field. Navigation and ultrasonic Doppler ultrasonography were essential. Angled endoscopes allowed more successful removal of tumors under direct visualization extending into the cavernous sinus and lower clivus. If cerebrospinal fluid (CSF) leakage occurred during operation, the dural opening was covered with a vascularized mucoseptal flap obtained from the nasal septum. Lumbar drainage system to prevent postoperative CSF rhinorrhea was frequently not required. Angled suction tips, single-shaft coagulation tools, and slim and longer holding forceps, all of which were newly designed for endoscopic surgery, were essential for smoother procedures. Endonasal endoscopic pituitary surgery allows less invasive transsphenoidal surgery since no postoperative nasal packing and less dependence on lumbar drainage are needed. Endoscopic pituitary surgery will be more common and become a standard procedure. Endoscopic skull base surgery has enabled more aggressive removal of extrasellar tumors with the aid of nasal and skull base techniques. Postoperative CSF leakage is now under control due to novel methods which have been proposed to close the dural defect in a water-tight manner. Endoscopic skull base surgery is more highly specialized, so needs special techniques and surgical training. Patient selection is also important, which needs collaboration with ear, nose, and throat specialists. As a safe and successful procedure in skull base surgery, this complex procedure should be carried out only in specialized hospitals, which deal with many patients with skull base lesions.

Key words: endoscope, pituitary tumor, skull base surgery

Introduction

Endoscopic endonasal transsphenoidal surgery has advantages such as less invasive surgical management and more aggressive tumor removal of extrasellar lesions.[6,10,11,14,16,17] In 2003, we began endoscope-assisted surgery.[16,17] In 2006, we completely switched to the endoscopic endonasal approach without using the operating microscope or nasal speculum.[16,17] Here we describe the procedures of endoscopic pituitary and skull base surgery in our institute.

Preoperative Imaging Studies

Preoperative evaluation of the nasal cavity is important to obtain images of the surgical field. Computed tomography (CT) evaluation of the lateral nasal cavity is one such preoperative procedure.[16] The extent of pneumatization of the sphenoid sinus is one of the factors to determine accessibility to the sella turcica. The CT slice parallel to the transsphenoidal approach is useful to show the anatomical structures of the nasal cavity and its surrounding structures.[16] The ethmoid sinus structures such as the middle nasal concha, uncinate process, ethmoid bulla, posterior ethmoid sinus, and superior nasal concha can be excised to gain a wider surgical corridor at the common nasal pathway.[17] Well-developed and pneumatized concha bullosa is a rather easy shape of the nasal cavity to gain a wider surgical corridor at the nasal cavity by lateralizing and pressing away from the nasal passage. Reconstruction of bone CT is useful for education of trainees, to

preoperatively imagine the anatomy and imitate the surgical procedure.

Instruments

Endoscopes with 0, 30, and 70 degrees should be prepared. Angled endoscopes are not easy to handle for trainees. However, by making the best use of angled endoscopes, we can gain access to and manipulate lesions which are difficult to approach under the operating microscope. Surgical instruments useful for endoscopic surgery include the rotating Kerrison punch, single-shaft bipolar coagulator, high speed drill, angled aspirator, cut through forceps, alligator forceps, and dissecting forceps. Long, angled, rotating, single-shafted tools are mandatory. The same positioning as in surgery under the operating microscope is used. The head is tilted to the contralateral side.

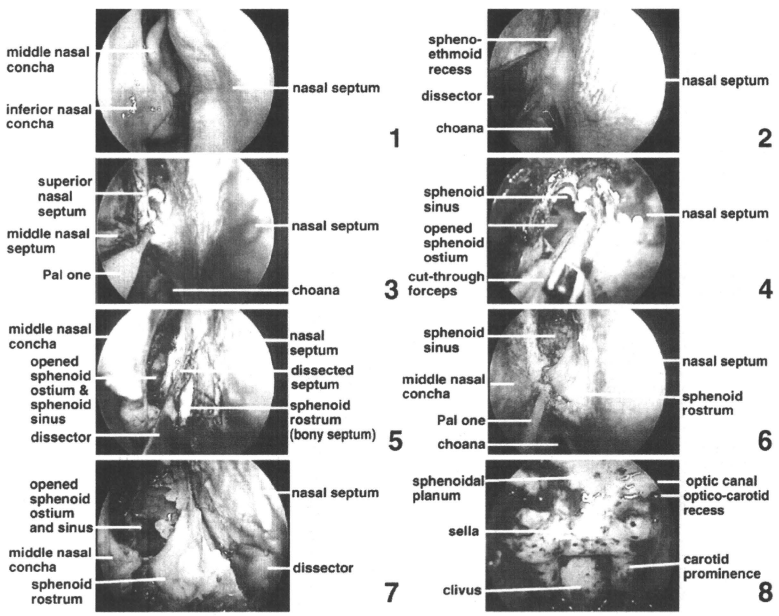

Fig. 1 With the 0 degree endoscope located at the upper part of the nose, the right nasal cavity is observed. Usually the inferior and middle nasal conchas come into view.
Fig. 2 To gain a view of the common nasal pathway, lateralization of the middle nasal concha is needed. After lateralization, the sphenoid ostium becomes visible at the sphenoethmoid recess. In this case, the ostium is underdeveloped.
Fig. 3 After confirming the location of the sphenoid ostium, coagulation of the mucosa around the sphenoid ostium is carried out.
Fig. 4 The sphenoid ostium is enlarged with the cut-through forceps.
Fig. 5 After coagulation of the mucosa, the mucous membrane is dissected on the nasal septum side.
Fig. 6 Septal mucosa is coagulated to avoid intra- and postoperative bleeding from the nasal mucosa.
Fig. 7 The sphenoid rostrum and vomer are visible.
Fig. 8 After removing the sphenoid rostrum and the mucosa of the sphenoid sinus, a panoramic view is obtained of the sella turcica, clivus, carotid prominences, optico-carotid recess, optic canal, and planum sphenoidale.

Standard Unilateral Approach

With the 0 degree endoscope placed at the upper part of the nostril, the inferior and middle nasal conchas usually come into view (Fig. 1). To gain a view of the deeper common nasal pathway, lateralization of the middle nasal concha is needed (Fig. 2). After lateralization, the sphenoid ostium becomes visible at the bottom of the sphenoethmoid recess. The size of the sphenoid ostium varies. In the well-pneumatized sphenoid sinus, the sphenoid ostium is large and clearly visible. Reoperated cases usually have an enlarged ostium. After confirming the location of the sphenoid ostium, coagulation of the surrounding mucosa is carried out (Fig. 3). Then, the sphenoid ostium is enlarged with the cut-through forceps (Fig. 4). After coagulation of the mucosa, the mucous membrane is dissected on the nasal septum side (Fig. 5). Dissected septal mucosa needs sufficient coagulation to confirm hemostasis (Fig. 6). The sphenoid rostrum and vomer then become visible (Fig. 7). The left sphenoid ostium is identified by dissecting the contralateral mucosa of the nasal septum. After exposing the rostrum of the sphenoid sinus, it is drilled and removed. After removing the mucosa in the sphenoid sinus, we obtain a panoramic view of the sella turcica, clivus, carotid prominences, and tuberculum sellae (Fig. 8). Identification of the opticocarotid recess shows sufficient exposure on the lateral side. The inferior side of the sella turcica needs to be drilled away toward the clivus. This procedure helps to gain an upward view with the angled scopes. After such a procedure, the dura is exposed (Fig. 9).

The dura is opened widely in a plus-shaped or x-shaped manner and the tumor is removed with a ring-curette (Fig. 10). The dura at the dorsum sellae becomes visible (Fig. 11). Angled endoscopes are useful to identify the surrounding structures such as the medial wall of the cavernous sinus in order not to overlook residual adenoma (Fig. 11). The highly angled (70 degrees) endoscope is used to explore the

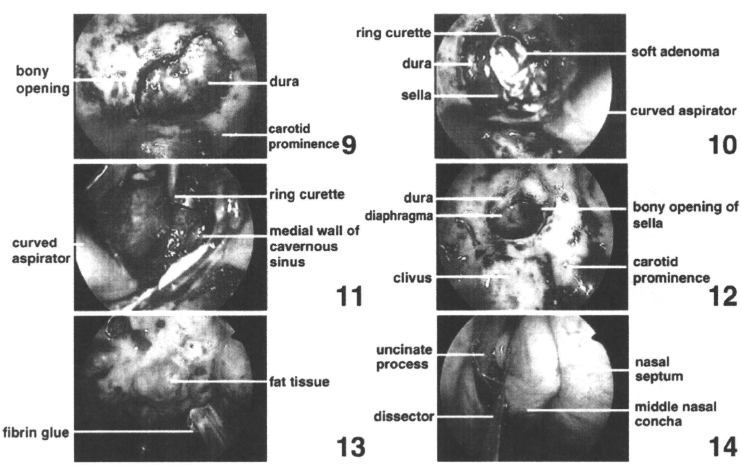

Fig. 9 The bony structure at the sellar floor is drilled away and the dura is exposed. This case is a growth hormone-secreting microadenoma.

Fig. 10 The dura is opened in a plus-shaped or x-shaped manner and removal of the tumor is carried out with a ring-curette.

Fig. 11 A 30-degree angled endoscope is useful to identify the surrounding structures such as the medial wall of the cavernous sinus in order not to overlook the residual adenoma.

Fig. 12 Total removal of the tumor is confirmed when the surrounding normal structures in the sella such as the residual normal gland, the arachnoid membrane, and diaphragm become visible.

Fig. 13 Abdominal fat is packed to fill the cavity. Fibrin glue is applied to stabilize the fat at the dural defect.

Fig. 14 The middle nasal concha is medialized to narrow the enlarged sphenoid ostium.

residual adenoma around the tuberculum sellae. Total removal of the tumor is confirmed by the surrounding structures in the sella such as the residual normal gland, arachnoid membrane, and diaphragm (Fig. 12).

The sellar floor is reconstructed with fat. The abdominal fat is packed to fill the cavity. Fibrin glue is applied to stabilize the fat at the dural defect (Fig. 13). The middle nasal concha is medialized to narrow the enlarged sphenoid ostium (Fig. 14).

Extended Approach

The extended approach is usually carried out for giant pituitary adenomas, craniopharyngiomas, tuberculum sellae meningiomas, and clival chordomas. The binasal approach is chosen. In order to carry out the approach comfortably and smoothly, we perform various procedures to widen the surgical corridor including middle nasal conchotomy, superior nasal conchotomy, removal of uncinate process and ethmoid bulla, and posterior ethmoidectomy, singly or combination. Several representative cases of extrasellar lesions are presented below.

Giant pituitary adenoma extending into the third ventricle: A 67-year-old woman presented with chief complaints of recent memory loss and visual field narrowing. She had undergone conventional transsphenoidal surgeries twice, craniotomy, and conventional radiotherapy. Malignant change of the pituitary adenoma was suspected clinically. T_1-weighted magnetic resonance (MR) imaging with contrast enhancement of this recurrent giant pituitary adenoma revealed the tumor extending to the level of the foramen of Monroe (Fig. 15). Superior and middle nasal conchotomies were performed. The tumor in the sella and suprasellar portions was soft and removable. At the final parts of the tumor removal, the 70-degree angled endoscope showed the anterior third ventricle (Fig. 16). The residual adenoma was aspirated. The panoramic view of the 30-degree angled endoscope showed the middle and posterior part of the third ventricle. The fornix, foramen of Monroe, choroid plexus, massa intermedia, and structures of the ventricle and aqueduct were visible (Fig. 17). Postoperative MR imaging with contrast enhancement one month after the surgery showed that the main mass lesion was excised. Temozolomide was effective to control the residual tumor.

Suprasellar craniopharyngioma: A 43-year-old

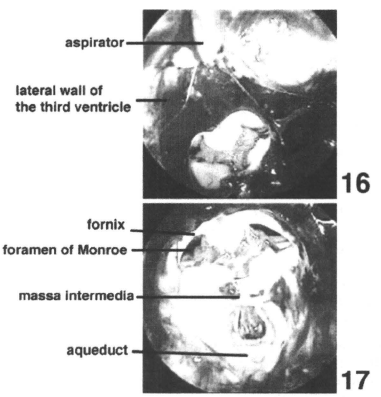

Fig. 16 After removal of the lower half of the tumor, the 70-degree angled endoscope shows the anterior third ventricle floor. The residual adenoma was aspirated.
Fig. 17 Panoramic view of the 30-degree angled endoscope. The middle and posterior parts of the third ventricle were visible. The fornix, foramen of Monroe, choroid plexus, massa intermedia, and aqueduct were visible.

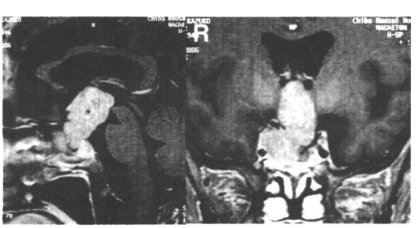

Fig. 15 T_1-weighted magnetic resonance images with contrast enhancement show the sellar and suprasellar giant pituitary adenoma extending to the level of the foramen of Monroe.

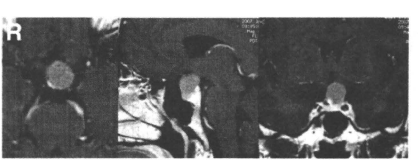

Fig. 18 T_1-weighted magnetic resonance images with contrast enhancement showing the cystic craniopharyngioma in the left suprasellar region, 15 mm in size, with slight enhancement of the right inferior portion.

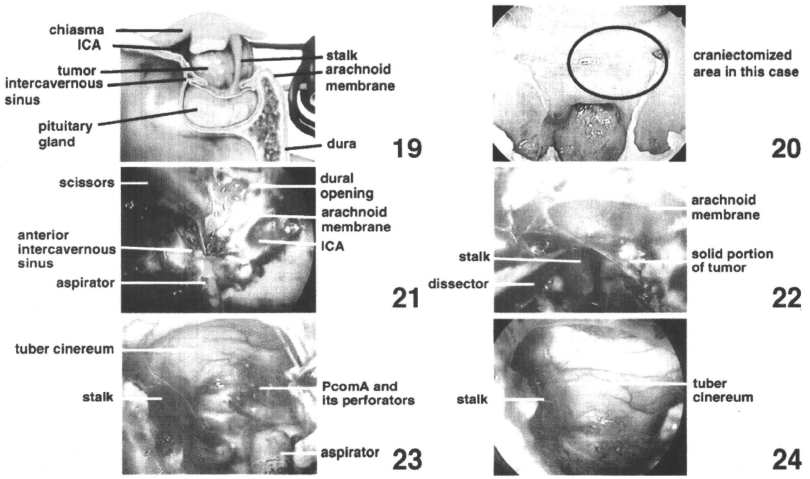

Fig. 19 Preoperative illustration demonstrating the tumor in relation to the dura, anterior intercavernous sinus, arachnoid membrane, and pituitary gland. The tumor was on the diaphragm sellae, and the optic chiasm and left optic nerve were compressed upward. ICA: internal carotid artery.

Fig. 20 Autopsy specimen showing the craniectomized area encircled in a *black line*.

Fig. 21 After bony removal at the sellar wall and tuberculum sellae area and dural opening, the anterior intercavernous sinus was coagulated and incised. ICA: internal carotid artery.

Fig. 22 Cyst content was aspirated and the cyst membrane was dissected from the surrounding structures. The pituitary stalk was visible and the tumor adhered to its lower part.

Fig. 23 After cyst wall removal, the posterior communicating artery (PcomA) and its perforators became visible. The tumor origin was located at the junction of the stalk and upper surface of the pituitary gland.

Fig. 24 The 30-degree endoscope was useful to observe the subchiasmal area such as the stalk and tuber cinereum.

man presented with a chief complaint of left visual field defect. He had noticed headache and left visual field disturbance for the last few days. T_1-weighted MR imaging with contrast enhancement showed the cystic mass lesion in the left suprasellar region, 15 mm in size, with slight enhancement of the right inferior portion (Fig. 18). Craniopharyngioma was suspected. Preoperative neuroimaging demonstrated the tumor in relation to the dura, anterior intercavernous sinus, arachnoid membrane, and pituitary gland. The tumor was on the diaphragm sellae, and the optic chiasm and left optic nerve were compressed upward (Fig. 19). The extended approach was chosen. The autopsy showed the craniectomized area in this case (Fig. 20). After bony removal at the sellar wall and tuberculum sellae area, the anterior intercavernous sinus was coagulated and incised (Fig. 21). Cyst content was aspirated and cyst membrane was dissected from the surrounding structures. The pituitary stalk was visible and the tumor adhered to its lower part around the diaphragm (Fig. 22). After cyst wall removal, the posterior communicating artery and its perforators became visible. The tumor origin was located at the junction of the stalk and upper surface of the pituitary gland (Fig. 23). The 30-degree endoscope was useful to observe the subchiasmal area such as the stalk and tuber cinereum. The angled endoscope provided an excellent surgical view of the subchiasmal region (Fig. 24). The sellar floor was reconstructed with fat tissue. Postoperatively the visual field defect disappeared. T_1-weighted MR imaging one month after the surgery showed successful removal of the tumor.

Tuberculum sellae meningioma: A 43-year-old woman complained of left visual field defect for several months. T_1-weighted MR imaging showed a homogeneous mass lesion in the suprasellar area on

the left. Tuberculum sellae meningioma was suspected (Fig. 25). Black and white reversed T_2-weighted MR imaging demonstrated the tumor intensity extending into the left optic canal in both axial and coronal images. Preoperative neuroimaging demonstrated the tumor in relation to the dura, arachnoid membrane, and pituitary gland (Fig. 26). The tumor was supposed to extend into the optic canal. The patient underwent binasal endonasal surgery. The autopsy demonstrated the craniectomized area in this case (Fig. 27). The left optic canal was opened to full length. After dural opening, the solid and hard tumor was internally decompressed. The tumor was resected from the dural attachment around the tuberculum sellae. The tumor invading the dura at the optic canal was incised with scissors and excised with the cut-through forceps (Fig. 28). The tumor extending into the optic canal was totally removed. The left optic canal was opened and the full length of the optic nerve was exposed (Fig. 29). The sellar floor was reconstructed with fat. Lumbar drainage was placed for one week postoperatively. T_1-weighted MR imaging one month after the surgery demonstrated that the mass was removed. The visual symptom disappeared postoperatively.

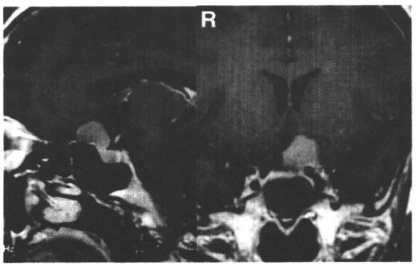

Fig. 25 T_1-weighted magnetic resonance images showing the homogeneous tuberculum sellae meningioma in the left suprasellar area.

Sellar Floor Reconstruction

Endoscopic endonasal approaches for ventral skull base lesions have evolved in the past decade. With these endoscopic developments, many pathologies can be treated within the intra-arachnoidal space, avoiding brain retraction and not requiring excessive neurovascular manipulations.[4,6,10,12,14] However, one of the challenges of endoscopic endonasal skull base approaches is the reconstruction of large defects of the skull base.[5] Various endoscopic techniques have been described to reconstruct the ventral skull base for preventing cerebrospinal fluid

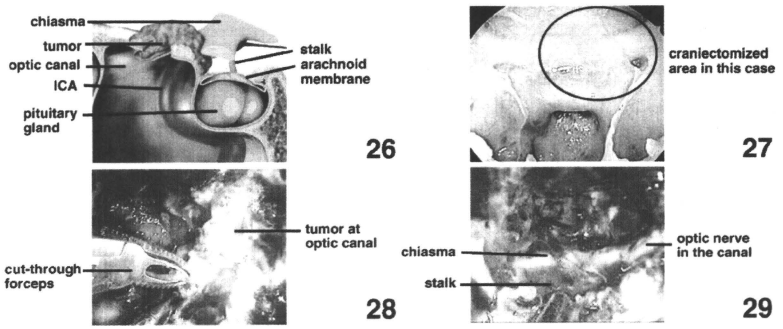

Fig. 26 Preoperative schema demonstrating the tumor in relation to the dura, arachnoid membrane, and pituitary gland. ICA: internal carotid artery.
Fig. 27 Autopsy specimen demonstrating the craniectomized area encircled in a *black line*.
Fig. 28 The left optic canal was opened to full length. After dural opening, the solid and hard tumor was internally decompressed. The tumor was excised with cut-through forceps from the dural attachment around the tuberculum sellae. The tumor extending into the optic canal was totally removed.
Fig. 29 The final view of the surgical field. The left optic canal was opened and the optic nerve in the optic canal was exposed.

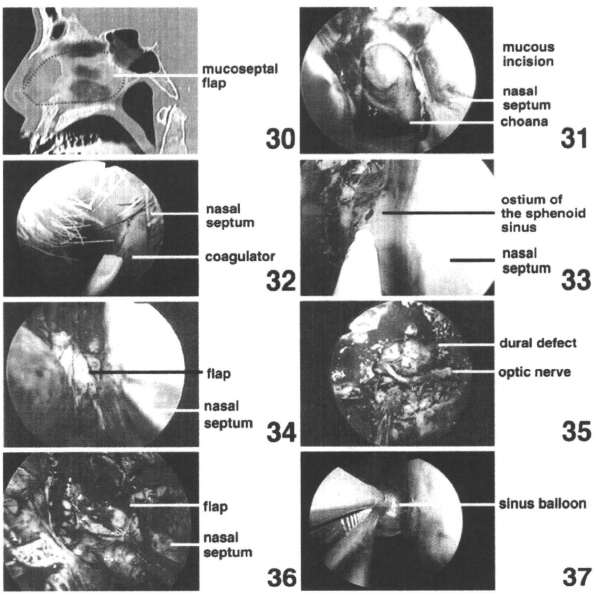

Fig. 30 The design to harvest the nasal septal flap is shown. The mucoperichondrial flap is based on the posterior septal branch of sphenopalatine artery.
Fig. 31 The vertical mucous incision is made at the medial side of the nasal septum around the choana. The incision is extended anteriorly to the base of the nasal cavity.
Fig. 32 The anterior vertical incision is made at the mucocutaneous junction at the nasal septum with unipolar electrocautery.
Fig. 33 The incision at the sphenoid ostium is made superiorly.
Fig. 34 The nasal septal flap is usually placed in the nasopharynx or the maxillary sinus until use in reconstruction.
Fig. 35 There is a large dural defect after removal of the tuberculum sellae meningioma.
Fig. 36 In the reconstruction phase, the nasal septal flap is laid directly on the large dural defect. Fibrin glue is used to avoid translocation of the flap.
Fig. 37 A sinus balloon catheter is finally placed as support.

(CSF) leaks, and can be divided into 4 methods: Conventional sellar floor reconstruction using autografts such as fat, muscle, fascia lata, and bone, and artificial grafts such as neo-veil, Surgicel, and others[1,16]; dural suturing with or without dural substitute[13]; the vascularized mucoseptal flap method[7-9,11]; and the multilayer method using dural and bony substitute.[2,3,15] Those methods are used singly or in combination as required by the practical situation.

We previously used fat grafts or fascia lata with insertion of external lumber drains for closure of large dural defects after endoscopic endonasal skull base approaches. Recently, we have adapted the use of the nasal septal flap vascularized by the posterior septal branch of sphenopalatine artery combined with a balloon catheter without insertion of lumbar drainage for closure of large dural defects.[9] Here we describe our surgical technique using a nasal septal flap combined with a balloon catheter. First we decide the design to harvest the nasal septal flap as a mucoperichondrial flap based on the posterior septal branch of sphenopalatine artery (Fig. 30). The middle nasal turbinate is usually dissected for

facilitating visualization from the nasal septum to the pedicle of the flap. The sphenoid ostium is easily identified and the flow in the donor artery of the flap is usually confirmed with a micro-Doppler probe. Then, the first incision is performed along the floor of the nasal cavity from the choanae to the intercutaneomucous point of the nasal vestibule with unipolar electrocautery (Fig. 31). The nasal septum is infiltrated with 1% lidocaine with epinephrine in a 1/250,000 ratio for hemostasis. The anterior vertical incision is made with unipolar electrocautery or turbinate scissors (Fig. 32) and the superior incision to the sphenoid ostium is made (Fig. 33). The incision is extended within 1.0–1.5 cm below the most superior aspect of the nasal septum. The mucosa of the nasal septum is elevated with a dissector. The pedicle of the flap formed in the width from the sphenoid ostium to the choana is extended laterally to the level of the sphenopalatine foramen. The nasal septal flap is usually placed in the nasopharynx or the maxillary sinus until use in reconstruction (Fig. 34). In the reconstruction phase, the nasal septal flap is laid directly on the large dural defect with fibrin glue (Figs. 35 and 36). Fat grafts are applied outside the flap as reinforcements. A sinus balloon catheter is finally placed as support (Fig. 37). Postoperative CT is performed on the 1st and 7th postoperative days to assess for postoperative hemorrhage, positions of the flap and the balloon catheter. External lumber drains are not inserted. Prophylactic intravenous antibiotics are administered for 7–10 days after surgery. Otorhinolaryngological endoscopic assessments are regularly performed at outpatient clinics.

Conclusion

Endonasal endoscopic pituitary surgery now allows less invasive transsphenoidal surgery without postoperative nasal packing and less dependence on lumbar drainage. Endoscopic pituitary surgery will be more common and become a standard procedure. Endoscopic skull base surgery has enabled more aggressive removal of extrasellar tumors with the aid of nasal and skull base techniques. Recent development of several tight dural closure methods helps to reduce postoperative CSF leakage. Such endoscopic skull base surgery is more highly specialized, so needs special techniques and surgical training. Patient selection is also important, which requires collaboration with ear, nose, and throat specialists. To be acknowledged as a safe and successful procedure in skull base surgery, this complex procedure should preferably be carried out only in specialized hospitals, which deal with many patients with skull base lesions.

References

1) Cappabianca P, Cavallo LM, Mariniello G, de Divitiis O, Romero AD, de Diviitis E: Easy sellar reconstruction in endoscopic endonasal transsphenoidal surgery with polyester-silicone dural substitute and fibrin glue: Technical note. *Neurosurgery* 49: 473–476, 2001
2) Castelnuovo PG, Delu G, Locatelli D, Padoan G, Bernardi FD, Pistochini A, Bignami M: Endonasal endoscopic duraplasty: Our experience. *Skull Base* 16: 19–24, 2006
3) Cavallo LM, Messina A, Esposito F, de Divitiis O, Dal Fabbio M, de Divitiis E, Cappabianca P: Skull base reconstruction in the extended endoscopic transsphenoidal approach for suprasellar lesions. *J Neurosurg* 107: 713–720, 2007
4) Couldwell WT, Weiss MH, Rabb C, Liu JK, Apfelbaum RI, Fukushima T: Variations on the standard transsphenoidal approach to the sellar region, with emphasis on the extended approaches and parasellar approaches: Surgical experience in 105 cases. *Neurosurgery* 55: 539–550, 2004
5) Esposito F, Dusick JR, Fatemi N, Kelly DF: Graded repair of cranial base defects and cerebrospinal fluid leaks in transsphenoidal surgery. *Neurosurgery* 60(4 Suppl 2): 295–304, 2007
6) Frank G, Pasquini E, Doglietto F, Mazzatenta D, Sciarretta V, Farneti G, Calbucci F: The endoscopic extended transsphenoidal approach for craniopharyngiomas. *Neurosurgery* 59 (1 Suppl 1): ONS75–ONS83, 2006
7) Hadad G, Bassagasteguy L, Carrau RL, Mataza JC, Kassam A, Snyderman CH, Mintz A: A novel reconstructive technique after endoscopic expanded endonasal approaches: Vascular pedicle nasoseptal flap. *Laryngoscope* 116: 1882–1886, 2006
8) Harvey RJ, Nogueira JF, Schlosser RJ, Patel SJ, Vellutini E, Stamm AC: Closure of large skull base defects after endoscopic transnasal craniotomy. *J Neurosurg* 111: 371–379, 2009
9) Horiguchi K, Murai H, Hasegawa Y, Hanazawa T, Yamakami Y, Saeki N: Endoscopic endonasal skull base reconstruction using a nasal septal flap; surgical results and comparison with previous reconstructions. *Neurosurg Rev* 33: 235–241, 2010
10) Kassam AB, Gardner P, Snyderman C, Mintz A, Carrau R: Expanded endonasal approach: fully endoscopic, completely transnasal approach to the middle third of the clivus, petrous bone, middle cranial fossa, and infratemporal fossa. *Neurosurg Focus* 19(1): E6, 2005
11) Kassam AB, Thomas A, Carrau RL, Snyderman CH, Vescan A, Prevedello D, Mintz A, Gardner P: Endoscoipc reconstruction of the cranial base using a pedicled nasoseptal flap. *Neurosurgery* 63(1 Suppl 1): ONS44-ONS53, 2008
12) Kato T, Sawamura Y, Abe H, Nagashima M: Transsphenoidal-transtuberculum sellae approach for

supradiaphragmatic tumors: Technical note. *Acta Neurochir (Wien)* 140: 715–719, 1998
13) Kitano M, Taneda M: Subdural patch graft technique for watertight closure of large dural defects in extended transsphenoidal surgery. *Neurosurgery* 54: 653–661, 2004
14) Laws ER, Kanter AS, Jane JA Jr, Dumont AS: Extended transsphenoidal approach. *J Neurosurg* 102: 825–828, 2005
15) Locatelli D, Rampa F, Acchiardi I, Bignami M, De Bernardi F, Castelnuovo P: Endoscopic endonasal approaches for repair of cerebrospinal fluid leaks: nine-year experience. *Neurosurgery* 58(4 Suppl 2): ONS246–ONS257, 2006
16) Saeki N, Murai H, Hasegawa Y, Horiguchi K, Hanazawa T: [Endoscopic endonasal transsphenoidal surgery for pituitary adenomas]. *No Shinkei Geka* 35: 971–985, 2007 (Japanese)
17) Saeki N, Murai H, Hasegawa Y, Horiguchi K, Hanazawa T, Fukuda K: [Endoscopic endonasal surgery for extrasellar tumors: Case presentation and its future perspective]. *No Shinkei Geka* 37: 229–246, 2009 (Japanese)

Address reprint requests to: Naokatsu Saeki, M.D., Department of Neurosurgery, Chiba University Graduate School of Medicine, 1–8–1 Inohana, Chuoh-ku, Chiba 260–8670, Japan.
e-mail: nsaeki@faculty.chiba-u.jp

J Neurooncol (2010) 98:163–167
DOI 10.1007/s11060-010-0169-x

CLINICAL STUDY/PATIENT STUDY

Gamma knife surgery for 1–10 brain metastases without prophylactic whole-brain radiation therapy: analysis of cases meeting the Japanese prospective multi-institute study (JLGK0901) inclusion criteria

Toru Serizawa · Tatsuo Hirai · Osamu Nagano · Yoshinori Higuchi · Shinji Matsuda · Junichi Ono · Naokatsu Saeki

Received: 6 November 2009 / Accepted: 31 March 2010 / Published online: 22 April 2010

Abstract We evaluated the results of stereotactic radiosurgery (SRS) alone using gamma knife (GK) for selected patients with 1–10 brain metastases without prophylactic whole-brain radiation therapy (WBRT) among JLGK0901-eligible cases. Seven hundred seventy-eight consecutive cases meeting the following JLGK0901 study inclusion criteria were analyzed: (1) newly diagnosed brain metastases, (2) 1–10 brain lesions, (3) less than 10 cm^3 volume of the largest tumor, (4) less than 15 cm^3 total tumor volume, (5) no magnetic resonance (MR) findings of cerebrospinal fluid (CSF) dissemination, and (6) no impaired activity of daily living [<70 Karnofsky Performance Score (KPS)] due to extracranial disease. At initial treatment, all lesions were irradiated with SRS without upfront WBRT. Thereafter, enhanced magnetic resonance imaging (MRI) was applied every 2–3 months, and new distant lesions were appropriately retreated with SRS or WBRT. We divided patients according to tumor number: single lesion for group A (280 cases), 2 for group B (135), 3–4 for group C (148), 5–6 for group D (93), and 7–10 for group E (122). Differences among groups were compared in terms of overall, neurological, qualitative, and new-lesion-free survival (NLFS). Median age was 65 years (range 26–92 years). There were 505 men and 273 women. The primary organ was lung in 579 patients, gastrointestinal tract in 79, breast in 48, urinary tract in 34, and others/unknown in 38. Mean survival time was 0.72 years (0.83 years for 1, 0.69 years for 2, 0.69 years for 3–4, 0.59 years for 5–6, and 0.62 years for 7–10 metastases). On multivariate analysis, significant poor prognostic factors for overall survival (OS) were active systemic disease, poor (<70) initial KPS, and male gender. Neurological survival and qualitative survival at 1 year were 92.7% and 88.2%, respectively. NLFS at 6 months and 1 year were 69.8% and 43.8%, respectively. There were statistically significant differences in new lesion emergence between groups A and B and between groups B and C. SRS using GK provides excellent results in selected patients with 1–10 brain lesions, without prophylactic WBRT. This study revealed that brain lesion number has no effect on any of the four types of survivals, which is anticipated to be confirmed by the JLGK0901 study.

Keywords Metastatic brain tumor · Stereotactic radiosurgery · Gamma knife surgery · Whole-brain radiation therapy · Prospective multi-institute study

T. Serizawa (✉) · T. Hirai
Tokyo Gamma Unit Center, Tsukiji Neurological Clinic, Tokyo, Japan
e-mail: gamma-knife.serizawa@nifty.com

O. Nagano · S. Matsuda · J. Ono
Gamma Knife House, Chiba Cardiovascular Center, Ichihara, Japan

Y. Higuchi · N. Saeki
Department of Neurological Surgery, Chiba University, Chiba, Japan

Introduction

We have treated patients with multiple, even relatively numerous, brain metastases (up to 10 or 25) with stereotactic radiosurgery (SRS) using gamma knife (GK) without prophylactic whole-brain radiation therapy (WBRT) under the same local treatment protocol. We previously reported the effectiveness and limitations of our protocol [5–11]. According to a Japanese randomized controlled study reported by Aoyama et al. [1], the efficacy of SRS alone for 1–4 brain metastases has been established. However,

we GK surgeons have some doubts about this upper limit of only four. Therefore, the Japan Leksell Gamma Knife (JLGK) Society has planned a prospective multi-institute study (Japan Leksell Gamma Knife JLGK0901) for selected patients with 1–10 brain lesions. Herein, we introduce the JLGK study and the anticipated results.

Materials and methods

Among 1,918 patients with metastatic brain tumors treated by GKS from January 1998 through May 2009, 778 who satisfied the following six criteria were analyzed: (1) newly diagnosed brain metastases, (2) 1–10 brain lesions, (3) less than 10 cm^3 volume of the largest tumor, (4) less than 15 cm^3 total tumor volume, (5) no magnetic resonance (MR) findings of cerebrospinal fluid (CSF) dissemination, and (6) no impaired activity of daily living (ADL) (<70 KPS) due to extracranial disease. At initial treatment, all lesions were irradiated with SRS without upfront WBRT. Primary physicians determined chemotherapy protocols. Neurological evaluations and gadolinium-enhanced magnetic resonance imaging (MRI) were performed every 2–3 months at our hospital, or at the primary hospital for as long as possible and then sent to us for evaluation. Dates and causes of death and impaired ADL were documented by the patients' primary physicians. Control of the GKS-treated lesions was defined by absence of any significant increase in tumor diameter (<20%). The applied definitions of "tiny," "small," and "medium" were $\leq$1.0 cm^3, >1.0 but $\leq$4.0 cm^3, and >4.0 but $\leq$10.0 cm^3, respectively. Standard peripheral doses were 22 Gy in tiny, 21 Gy in small, and 20 Gy in medium-sized lesions. We changed the dose by $\pm$2 Gy depending on tumor pathology, physical status, tumor location, extracranial disease status, etc. Neurological death was defined as death due to all forms of intracranial disease, including tumor recurrence, carcinomatous meningitis, cerebral dissemination, and other unrelated intracranial diseases, as described by Patchell et al. [2]. Impaired ADL was defined as impaired neurological status as reflected by KPS <70 (functional preservation), as reported by Aoyama et al. [1]. Intervals from date of SRS treatment until date of death (overall survival, OS), neurological death (neurological survival, NS), impaired ADL (qualitative survival, QS), and appearance of new distant lesions (new-lesion-free survival, NLFS) were calculated by Kaplan–Meier method. We divided patients according to tumor number: single lesion for group A (280 cases), 2 for group B (135), 3–4 for group C (148), 5–6 for group D (93), and 7–10 for group E (122). Differences among groups were compared in terms of OS, NS, QS, and NLFS. A probability value <0.01 was taken to represent a statistically significant difference.

Results

The distributions of patient and treatment factors are summarized in Table 1. Figure 1 shows cumulative tumor-progression-free survival curves according to tumor volume. Tumor control rates at 1 year were 98.4% in tiny, 92.3% in small, and 77.9% in medium-sized tumors. Differences were statistically significant ($p < 0.0001$). The peripheral dose applied to the tumor margin was 13.5–30 Gy [mean $\pm$ standard deviation (SD): 20.7 $\pm$ 1.1 Gy, median: 20 Gy] with a 57.6% isodose contour (range 36–95%). Mean prescribed doses were 21.6 Gy in 281 tiny, 21.1 Gy in 292 small, and 20.1 Gy in 207 medium-sized lesions. Among 70 control-failure lesions, which were clinically diagnosed as tumor recurrence in 38 and radiation injury in 32, surgical removal was required for 9 lesions (7 recurrence, 2 radiation injury).

Mean survival time (MST) was 0.72 years (0.83 years in group A, 0.69 years in group B, 0.69 years in group C, 0.59 years in group D, and 0.62 years in group E), as shown in Fig. 2. MST was 0.83 years in lung cancer, 0.65 years in gastrointestinal (GI) tract, 0.91 years in breast, 0.68 years in urinary tract, and 0.41 in other/unknown origin. There were no significant differences; p values were 0.1596 (A–B),

Table 1 Dichotomized patient characteristics

Characteristics		
Age (years)	Median	65
	Min–max	26–92
Sex	Male	505
	Female	273
Extracranial disease	Controlled	84
	Active	694
Pre-treatment KPS score	Median	100
	Min–max	60–100
Primary organ	Lung	579
	GI tract	79
	Breast	48
	Kidney	34
	Others	38
Number of brain lesions	Median	2
	Min–max	1–10
Maximum lesion volume (cm^3)	Median	1.8
	Min-max	0.1–9.9
Total tumor volume (cm^3)	Median	2.8
	Min–max	0.1–15.0
Metastasis	Synchronous	201
	Metachronous	577
RTOG-RPA classification	Class 1	34
	Class 2	694
	Class 3	50

KPS Karnofsky performance status, *CSF* cerebrospinal fluid

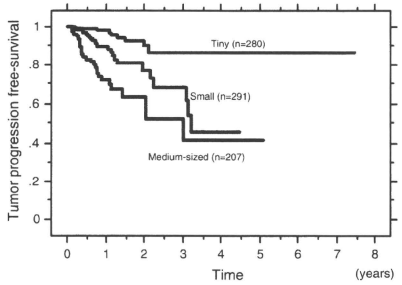

Fig. 1 Tumor-progression-free survival according to tumor volume. The tumor control rate at 1 year was 98.4% for tiny, 92.3% for small, and 77.9% for medium-sized tumors. Differences were statistically significant ($p < 0.0001$). The peripheral dose applied to the tumor margin was 13.5–30 Gy (mean ± SD: 20.7 ± 1.1 Gy, median: 20 Gy) with a 57.6% isodose contour (range 36–95%). Mean prescribed doses were 21.6 Gy in 281 tiny, 21.1 Gy in 292 small, and 20.1 Gy in 207 medium-sized lesions

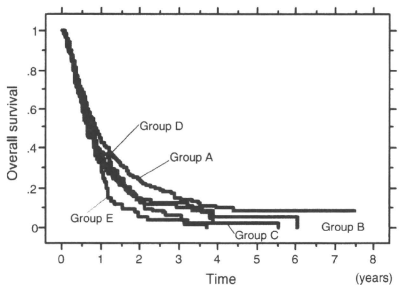

Fig. 2 Overall survival curves according to tumor number. Mean survival time (MST) was 0.72 years (0.83 years in group A, 0.69 years in group B, 0.69 years in group C, 0.59 years in group D, and 0.62 years in group E). There were no significant differences between any two groups; p values were 0.1596 (A–B), 0.2924 (B–C), 0.1594 (C–D), and 0.1050 (D–E)

0.2924 (B–C), 0.1594 (C–D), and 0.1050 (D–E), as shown in Table 2. On multivariate analysis, significant prognostic factors for OS were active extracranial disease [$p < 0.0001$, hazard ratio (HR) 2.994], low pretreatment KPS ($p = 0.0059$, HR 1.517), and male gender ($p < 0.0001$, HR 1.411). Overall survival curves are compared according to Radiation Therapy Oncology Group recursive partitioning analysis (RTOG-RPA) classes, as in Gasper's report [3], in Fig. 3. Mean survival periods were 2.2 years in class 1 ($n = 34$), 0.7 years in class 2 ($n = 694$), and 0.3 years in class 3 ($n = 50$). The differences among groups were statistically significant. Chemotherapy after SRS did not affect overall survival.

Table 2 p Values between pairs of groups

	A vs. B	B vs. C	C vs. D	D vs. E	C vs. E
OS	0.1596	0.2924	0.1594	0.1050	0.8073
NS	0.3860	0.0470	0.5162	0.8454	0.4816
QS	0.7606	0.0163	0.8184	0.6818	0.4142
NLSF	**0.0003**	**0.0047**	0.2905	0.0304	0.2061

Bold values represent statistically significant ($P < 0.01$)

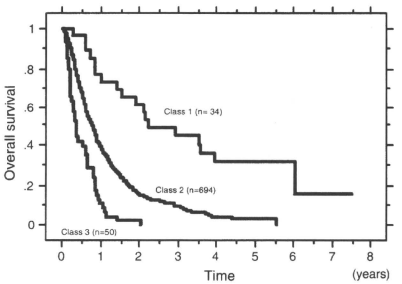

Fig. 3 Overall survival curves according to Radiation Therapy Oncology Group recursive partitioning analysis (RTOG-RPA) class. Mean survival was 2.2 years in class 1 ($n = 34$), 0.7 years in class 2 ($n = 694$), and 0.3 years in class 3 ($n = 50$). The differences among groups were statistically significant ($p < 0.0001$)

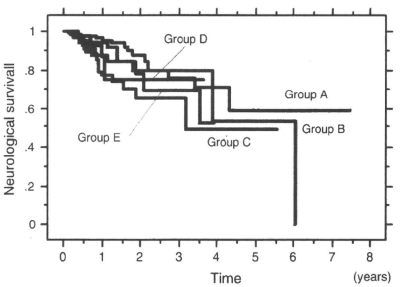

Fig. 4 Neurological survival curves according to tumor number. The neurological survival rate at 1 year was 96.8% in group A, 95.5% in group B, 84.7% in group C, 91.2% in group D, and 89.2% in group E. There were no significant differences between any two sequential groups

The neurological-death-free rate was 92.4% at 1 year and 82.5% at 2 years. Figure 4 shows NS curves according

to tumor number. The NS rate at 1 year was 96.8% in group A, 95.5% in group B, 84.7% in group C, 91.2% in group D, and 89.2% in group E. There were no significant differences between any two adjacent groups (Table 2). Functional-preservation-free survival curves are shown in Fig. 5. The QS rate was 87.8% at 1 year and 73.0% at 2 years in all cases. The functional-preservation-free rate at 1 year was 90.7% in group A, 93.3% in group B, 80.8% in group C, 84.3% in group D, and 85.8% in group E. There were no significant differences between any two sequential groups (Table 2). NLFS curves according to number of brain metastases are shown in Fig. 6. The new-distant-lesion-free rate at 1 year was 54.3%. The new-distant-lesion-free rate at 1 year was 71.6% in group A, 53.7% in group B, 43.6% in group C, 50.7% in group D, and 66.3% in group E. There were significant differences between groups A and B ($p = 0.0003$) and between groups B and C ($p = 0.0047$), as shown in Table 2.

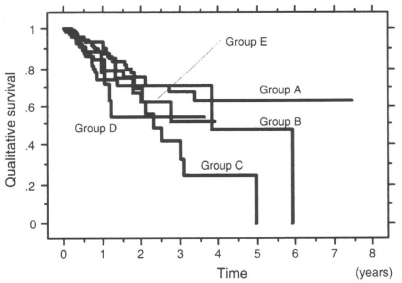

Fig. 5 Qualitative survival according to tumor number. The qualitative survival rate was 87.8% at 1 year and 73.0% at 2 years in all cases, and 90.7% in group A, 93.3% in group B, 80.8% in group C, 84.3% in group D, and 85.8% in group E. There were no significant differences between any two sequential groups

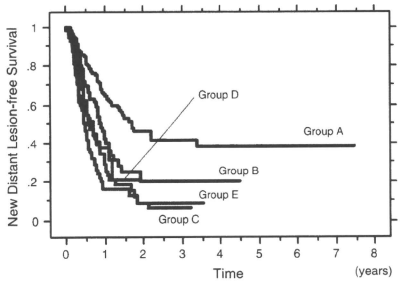

Fig. 6 New-lesion-free survival curves according to tumor number. The new-distant-lesion-free rate at 1 year was 54.3%. The new-distant-lesion-free rate at 1 year was 71.6% in group A, 53.7% in group B, 43.6% in group C, 50.7% in group D, and 66.3% in group E. There was significant difference between groups A and B ($p = 0.0003$) and also between groups B and C ($p = 0.0047$)

Discussion

Background of JLGK0901 study

The Japanese Radiation Oncology Study Group (JROSG) study reported by Aoyama [1] found no significant differences, in OS, NS or QS, between SRS alone and SRS with upfront WBRT, although new lesions and tumor progression were observed significantly more frequently with SRS alone. These results confirmed the efficacy of SRS alone for patients with 1–4 brain metastases. However, evidence supporting SRS alone for multiple brain tumors, i.e., exceeding 4, has not been established. Indeed, SRS using GK has been widely applied to multiple brain metastases, as reported especially by Japanese groups. Serizawa and Yamamoto [4–12] insisted that factors limiting SRS alone using GK include not only the number but also the size of lesions, presence of CSF dissemination, and total tumor volume. As the first step to filling the gap between broad clinical application and limited evidence for multiple brain tumors, we, the Japan Leksell Gamma Knife Society, planned a prospective multi-institute study of GK without upfront WBRT in selected patients with 1–10 brain metastases.

Introduction of JLGK0901 study

Based on the considerable experience and vast literature for GK alone in treating multiple brain metastases in Japan, the following intracranial conditions are not considered to be good indications for GK alone:

1. >10 cm^3 volume of the largest tumor
2. >15 cm^3 total tumor volume
3. Presence of CSF dissemination
4. Numerous (>10) brain metastases
5. Impaired ADL (<70 KPS) due to extracranial disease

Thus, the JLGK0901 study committee set the above as exclusion criteria. Cases with sarcoma, lymphoma, or cancer with unknown primary were also excluded. The protocol stipulates follow-up, including enhanced MRI and neurological examinations, at least every 3 months. Twelve hundred cases will be registered from 23 Japanese GK sites within 2 years, and a 1-year follow-up period will

be mandatory. This trial has been registered by the Japanese ethics committee (University Hospital Medical Information Network, UMIN 0000001812, http://www.umin.ac.jp/).

Expected results of the JLGK0901 study

In this retrospective study, all cases were eligible according to the inclusion criteria, and for the follow-up protocol, of the JLGK0901 study. Indeed, the results presented herein are attributable to our statistical base in the JLGK protocol. This prospective study is designed to prove the noninferiority of overall survival with several metastases in groups D and E versus 3–4 metastases in group C. With 80% statistical power, at the 0.025 level of probability (one sided), with a 2-year registration period, and 1-year follow-up after completion of registration, a planned total sample size of 1,200 has been determined for this prospective trial. Our experience leads us to conclude that the multiple brain metastases group (MST: 6.7 months) will not have results inferior to those of the oligo-brain metastases group (MST: 8.1 months) for 1-year survival with a noninferiority margin of 7.5% [13]. Noninferiority is confirmed if the upper limit of the confidence interval of the hazard ratio does not exceed the limit of 1.3, which is in accord with the non-inferiority margin.

If our present retrospective results for patients with more than 4 brain metastases being almost the same as those of patients with 3–4 brain lesions are valid, the efficacy of GK alone for 5–10 brain metastases is anticipated to be confirmed by the JLGK0901 study, which is a well-designed prospective multi-institute controlled trial. If this study proves equality between 3–4, 5–6, and 7–10 brain metastases, in terms of OS, NS, QS, and NLFS, level 2 evidence of the efficacy of GK without prophylactic WBRT for multiple brain metastases will be established.

Conclusions

In terms of OS, NS, QS, and NLFS, GK without upfront WBRT for 1–10 brain metastases from various primary cancers provides excellent palliation considering the patients' short life expectancies. The results for patients with more than 4 brain metastases were almost the same as those of patients with 3–4 brain lesions in our retrospective study. These results are anticipated to be confirmed by the JLGK0901 study, which is a well-designed prospective multi-institute controlled trial. If this study proves equality between 3–4, 5–6, and 7–10 brain metastases in terms of OS, NS, QS, and NLFS, level 2 or 3 evidence of the efficacy of GK alone for 5–10 brain metastases will be established.

References

1. Aoyama H, Shirato H, Tago M, Nakagawara K, Toyoda T, Hatano Kenjo M, Oya N, Hirota S, Shioura H, Kunieda E, Inomata T, Hayakawa K, Katoh N, Kobayashi (2006) Stereotactic radiosurgery plus whole brain radiation therapy vs stereotactic radiosurgery alone for treatment of brain metastases: a randomized controlled trial. JAMA 295(21):20535–20536
2. Patchell RA, Tibbs PA, Walsh JW, Dempsey RJ, Maruyama Y, Kryscio RJ, Markesbery WR, Macdonald JS, Young B (1990) A randomized trial of surgery in the treatment of single metastases to the brain. N Engl J Med 322:494–500
3. Gaspar L, Scott C, Rotman M, Asbell S, Phillips T, Wasserman T, Mc Kenna WG, Byhardt R (1997) Recursive partitioning analysis (RPA) of prognostic factors in three Radiation Therapy Oncology Group (RTOG) brain metastases trials. Int J Radiat Oncol Biol Phys 37:745–751
4. Serizawa T, Iuchi T, Ono J, Saeki N, Osato K, Odaki M, Ushikubo O, Sato M, Matsuda S (2000) Gamma knife treatment for multiple metastatic brain tumors compared with whole-brain radiation therapy. J Neurosurg 93(Suppl 3):32–36
5. Serizawa T, Ono J, Iuchi T, Matsuda S, Sato M, Odaki M, Hirai S, Sato K, Yamaura A (2002) Gamma knife radiosurgery for metastatic brain tumors from lung cancer. Comparison between small cell cancer and non-small cell cancer. J Neurosurg 97(Suppl 5):484–488
6. Serizawa T, Saeki N, Higuchi Y, Ono J, Iuchi T, Nagano O, Yamaura A (2005) Gamma knife surgery for brain metastases: indications for and limitations of a local treatment protocol. Acta Neurochir (Wien) 147:721–726
7. Serizawa T, Higuchi Y, Ono J, Matsuda S, Iuchi T, Nagano O, Saeki N (2006) Gamma knife surgery for metastatic brain tumors from lung cancer without prophylactic whole brain radiation therapy. In: Kondziolka D (ed) Radiosurgery. Karger, Basel, Switzerland, pp 186–198
8. Serizawa T, Higuchi Y, Ono J, Matsuda S, Nagano O, Iwadate Y, Saeki N (2006) Gamma knife surgery for metastatic brain tumor without prophylactic whole brain radiation therapy: results in 1000 consecutive cases. J Neurosurg 105:86–90
9. Serizawa T, Yamamoto M, Nagano O, Higuchi Y, Matsuda S, Ono J, Iwadate Y, Saeki N (2008) Gamma knife surgery for metastatic brain tumors. A 2-institute study in Japan. J Neurosurg 109:118–121
10. Serizawa T (2008) Metastatic brain tumors: lung cancer. In: Yamamoto M (ed) Japanese experience with gamma knife radiosurgery. Karger, Basel, Switzerland, pp 142–153
11. Yang CC, Ting J, Wu X, Markoe A (1998) Dose volume histogram analysis of gamma knife radiosurgery treating twenty-five metastatic intracranial tumors. Stereotactic Funct Neurosurg 70:41–49
12. Yamamoto M, Ide M, Nishio S, Urakawa Y (2002) Gamma knife radiosurgery for numerous brain metastases: is this a safe treatment? Int J Radiat Oncol Biol Phys 53(5):1279–1283
13. Schoenfeld DA, Richter JR (1982) Nomograms for calculating the number of patients needed for a clinical trial with survival as an endpoint. Biometrics 38(1):163–170

Sato *et al. Health and Quality of Life Outcomes* 2010, **8**:38
http://www.hqlo.com/content/8/1/38

HEALTH AND QUALITY OF LIFE OUTCOMES

RESEARCH

Open Access

Development of the Japanese version of the Pediatric Quality of Life Inventory™ Brain Tumor Module

Iori Sato[1], Akiko Higuchi[2], Takaaki Yanagisawa[3], Akitake Mukasa[4], Kohmei Ida[5], Yutaka Sawamura[6], Kazuhiko Sugiyama[7], Nobuhito Saito[4], Toshihiro Kumabe[8], Mizuhiko Terasaki[9], Ryo Nishikawa[10], Yasushi Ishida[11] and Kiyoko Kamibeppu*[1]

Abstract

Background: The Pediatric Quality of Life Inventory™ (PedsQL™) is a widely-used modular instrument for measuring health-related quality of life in children aged 2 to 18 years. The PedsQL™ Brain Tumor Module is comprised of six scales: Cognitive Problems, Pain and Hurt, Movement and Balance, Procedural Anxiety, Nausea, and Worry. In the present study, we developed the Japanese version of the PedsQL™ Brain Tumor Module and investigated its feasibility, reliability, and validity among Japanese children and their parents.

Methods: Translation equivalence and content validity were verified using the standard back-translation method and cognitive debriefing tests. Participants were recruited from 6 hospitals in Japan and the Children's Cancer Association of Japan, and questionnaires were completed by 137 children with brain tumors and 166 parents. Feasibility of the questionnaire was determined based on the amount of time required to complete the form and the percentage of missing values. Internal consistency was assessed using Cronbach's coefficient alpha. Test-retest reliability was assessed by retesting 22 children and 27 parents. Factorial validity was verified by exploratory factor analyses. Known-groups validity was described with regard to whole brain irradiation, developmental impairment, infratentorial tumors, paresis, and concurrent chemotherapy. Convergent and discriminant validity were determined using Generic Core Scales and State-Trait Anxiety Inventory for children.

Results: Internal consistency was relatively high for all scales (Cronbach's coefficient alpha > 0.70) except the Pain and Hurt scale for the child-report, and sufficient test-retest reliability was demonstrated for all scales (intraclass correlation coefficient = 0.45-0.95). Factorial validity was supported through exploratory factor analysis (factor-item correlation = 0.33-0.96 for children, 0.55-1.00 for parents). Evaluation of known-groups validity confirmed that the Cognitive Problems scale was sensitive for developmental impairment, the Movement and Balance scale for infratentorial tumors or paresis, and the Nausea scale for a patient currently undergoing chemotherapy. Convergent and discriminant validity with the PedsQL™ Generic Core Scales and State-Trait Anxiety Inventory for children were acceptable.

Conclusions: The Japanese version of the PedsQL™ Brain Tumor Module is suitable for assessing health-related quality of life in children with brain tumors in clinical trials and research studies.

Background

Five-year survival rates for pediatric brain tumor patients are approaching 70% [1], and with this increasing survival rate comes the challenge of improving these patients' overall quality of life. Children undergoing treatment for these tumors often show several typical symptoms, such as pain, nausea, and a lack of energy [2]. Further, even after treatment has ended, consequences to the original tumor or this therapy remain, including neurological and endocrinological problems [3-5]. Among long-term survivors, cognitive problems and difficulties with psychosocial adjustment have been reported years after treatment

* Correspondence: kkamibeppu-tky@umin.ac.jp

[1] Department of Family Nursing, Graduate School of Health Sciences and Nursing, Faculty of Medicine, The University of Tokyo, 7-3-1 Hongo, Bunkyo-ku, Tokyo 113-0033, Japan

Full list of author information is available at the end of the article

[3-8]. Other studies have also noted further evidence supporting the notion that children with brain tumors experience generally lower health status and quality of life than children afflicted with other malignant diseases at all stages of their disease and recovery [9,10].

We can thus determine from these previous studies that indices for endpoints secondary to survival are necessary to improve quality of life among these patients, and to this end, clinicians and researchers have turned their focus to health-related quality of life (HRQOL) [11]. HRQOL is a continuous concept influenced by a person's objective assessments of function or health status as well as subjective perceptions of their personal health [12]. The domain set for HRQOL, such as physical, emotional, and cognitive domains, varies according to an individual's characteristics, such as age and disease. Several widely-used measurements specific to assessing HRQOL in patients with brain tumors have been developed already, including Functional Assessment of Cancer Therapy - Brain Subscale [13] and European Organisation for Research and Treatment Center Quality of Life Questionnaire - Brain Caner Module [14], but these methods are not suitable for use on children. To measure HRQOL among children with brain tumors, we have used the Pediatric Quality of Life Inventory™ (PedsQL™) Generic Core Scales [15], which contain general domains but no brain tumor-specific domains. Taking into account this need for a more appropriate measurement, the PedsQL™ Brain Tumor Module [16] was developed as a PedsQL™ disease-specific module.

The PedsQL™ is a widely-used measurement of HRQOL in children aged 2-18 years [15]. Reports are conducted bilaterally; children aged 5-18 are asked to evaluate their own HRQOL (child-report) and the parents of children aged 2-18 are asked to evaluate their child's HRQOL (parent-report). The PedsQL™ was designed under a modular-approach [17] to cover both generic and disease-specific domains. The PedsQL™ Brain Tumor Module was developed through focus groups involving healthcare providers, children, and parents; cognitive interviews; pre-testing; and field-testing [16]. We determined the PedsQL™ Brain Tumor Module to be highly appropriate for use in assessing HRQOL in children with brain tumors, who often suffer from dysfunction of higher cognitive abilities and visual and physical impairment [3,4], for three reasons. First, the module contains only 24 items, a number far fewer than other scales, thereby reducing the time required to complete the questionnaire. This relatively short questionnaire is ideal for administration to children, given their short attention spans when compared to adults. Second, the PedsQL™ protocol permits interviewer administration for children who have difficulty completing self-administered questionnaires [16,18], ideal for children with visual or motor impairments. Third, the module features several formats aimed at children across several age groups, including questionnaires for children aged 5-7 (young child), 8-12 (child), and 13-18 (adolescent) years. In comparison, the parent-report includes questionnaires for parents of children aged 2-4 (toddler), 5-7, 8-12, and 13-18 years. Although the format varies according to lifestyle and cognitive development level, the measured content and concepts are the same for all ages. This relatively wide age-range and comparability across age ranges allows us to simultaneously examine results across multiple age groups and longitudinally examine a specific-age group for a relatively long period of time.

In the present study, to facilitate the sharing of data across international borders, we developed the Japanese version of the PedsQL™ Brain Tumor Module and investigated its feasibility, reliability, and validity. Given the wide biological diversity exhibited by brain tumors, the number of patients available to participate in trials is invariably limited by the paucity of homogeneous groups in a single country [19]. Clinical trials and epidemiological studies on an international scale are therefore of the utmost importance, requiring feasible, reliable, and valid global indices.

Methods

Scale development

Permission was obtained from the rights holder, Dr. James W. Varni (JWV), to translate the PedsQL™ Brain Tumor Module into Japanese using a preassigned translation procedure [20]. Two Japanese translators proficient in English produced forward translations independent of one another. These forward translations were then discussed among the authors and translators, all of whom agreed on a single, reconciled version which was a conceptually equivalent translation of the original English version and written in easily understood language. An English translator proficient in Japanese and blinded to the original English version then translated this reconciled version back into English. After comparing the back-translated and original versions and making minor amendments to the reconciled version, we produced a pilot questionnaire.

Eight children with brain tumors participated in pilot testing along with their parents. A researcher (IS or AH) measured the time taken to complete the questionnaire. On completing the questionnaire, the researcher interviewed each child and his or her parent, and the thought processes used in answering the questionnaire were deduced by cognitive interviewing [21]. A final version of the Japanese version of the PedsQL™ Brain Tumor Module was produced after revising the pilot version using data obtained during pilot testing. JWV reviewed the

conceptual and linguistic equivalence between the final Japanese version and the original English version.

Study population

We recruited children with brain tumors and their parents from six hospitals across Japan and from the Children's Cancer Association of Japan (CCAJ), a non-profit organization established in 1968 which supports children with cancer and their families. Participants were recruited from September to December 2008. With regard to inclusion criteria, a child was included if he or she was aged 5 to 18 years, while the parent was included if his or her child was aged 2 to 18 years (age range covered by the PedsQL™). Families were included in the study if at least one month had passed since the child's brain tumor diagnosis. With regard to exclusion criteria, families were excluded from the study if hospital doctors or social workers of the CCAJ determined the family to be unsuitable for participating in the study due to finding the subject of brain tumors too painful to discuss.

Procedure

Researchers presented this study to 101 children and 122 parents at the participating hospitals both orally and in writing. Of these, 98 children and 120 parents elected to participate, providing informed consent or assent. At CCAJ, the study was described in writing to all families invited to a meeting regarding brain tumors. Of 55 responding families, 45 children and 52 parents provided informed consent or assent. Two of the families were bereaved, one had an adult survivor, six children were aged two to four years, and one child did not provide informed consent. In total, questionnaires were distributed to 143 children and 172 parents.

Child-report questionnaires were self- or interviewer-administered to participants. When providing informed consent, parents determined whether their child was able to self-administer the questionnaire. In accordance with the PedsQL™ administration guidelines, children aged 5-7 years or otherwise determined to be incapable of self-administration were administered the questionnaire by either a researcher or their parents reading the instructions and each item [15,16,18]. At the same time, parent-report questionnaires were self-administered to participants.

After administration, questionnaires were collected from 138 children and 167 parents, with 5 children and 5 parents not returning their questionnaires. One child and one parent were unable to answer the questionnaire (respective reasons are described in the Results section), and thus answers from 137 children and 166 parents were ultimately analyzed.

Retest reliability was assessed at the two hospitals located nearest to our study group's agency, and the details of the retest were explained to all 27 children and 31 parents enrolled in the initial study orally and in writing following completion of the initial questionnaire. After undergoing assessment by their attending physician, all children were determined to be stable. The same parents who completed the initial questionnaire were asked to complete the retest. In total, 24 children and 29 parents provided informed consent or assent. Participants were readministered the PedsQL™ Brain Tumor Module between 7 and 28 days (median = 9.5) after completion of the initial questionnaire. At the same time, we inquired into any changes in the child's physical condition or lifestyle during this period. Retest reliability was evaluated on exclusion of responses from either a child or a parent which reported changes in the child's physical condition or lifestyle during the period.

Measurements

The PedsQL™ Brain Tumor Module [16] is comprised of six scales: Cognitive Problems (seven items), Pain and Hurt (three items), Movement and Balance (three items), Procedural Anxiety (three items), Nausea (five items), and Worry (three items). The parent-report for toddlers (ages 2-4) does not include the Cognitive Problems scale, while the child- and parent-reports for young children (ages 5-7) list only six items on the Cognitive Problems scale.

Respondents are asked to describe the extent to which each item has troubled them over the past seven days. For the child-reports for ages 8-18 and all parent-reports, a 5-point Likert response scale is used (0 = never [a problem]; 1 = almost never; 2 = sometimes; 3 = often; 4 = almost always). For the child-report for children ages 5-7, a 3-point face response scale is used to aid participants in understanding the concept of rating scales. Items are reverse-scored and linearly transformed to a 0-100 scale, with higher scores indicating a better HRQOL. To account for missing data, scale scores are computed as the sum of the items divided by the number of items answered. If more than 50% of the items are missing or incomplete, the scale score is not computed. JWV's original version has acceptable construct validity and internal consistency (Cronbach's coefficient alpha [22] = 0.76-0.92).

The PedsQL™ Generic Core Scales [15] has four scales: Physical Functioning (eight items), Emotional Functioning (five items), Social Functioning (five items), and School Functioning (five items). The format, instructions, response scale, and scoring method are identical to the PedsQL™ Brain Tumor Module. The Japanese version of the PedsQL™ Generic Core Scales was developed by Kobayashi et al [23]. Internal consistencies for the Physical, Emotional, Social, and School Functioning scales for the child- and parent-reports in the current study were

0.84 and 0.92, 0.76 and 0.82, 0.74 and 0.89, and 0.73 and 0.77, respectively.

The State-Trait Anxiety Inventory for Children (STAIC) [24] is comprised of two scales: State Anxiety (20 items) and Trait Anxiety (20 items). Each scale is scored for children aged 8 or over on three levels of self-reported anxiety intensity, with a sum score between 20 and 60 and higher scores indicating increased anxiety. The Japanese version was developed by Soga [25]. Internal consistencies for the State and Trait Anxiety scales in the current study were 0.89 and 0.89, respectively.

Parents were also asked to describe their child's characteristics, namely the child's age, sex, tumor pathology, tumor location, age at diagnosis, experience with treatment, medical history, and existing complications. Parents were also questioned regarding what they believed their economic status to be, their age, their biological relationship to their child, and their academic background.

Statistical analyses

All analyses were performed using SPSS software, version 12.0J (SPSS, Inc., Chicago, Illinois, USA) and the level of significance set at 0.05. Missing values were considered by pair-wise case deletion. Score distributions for the Japanese version of the PedsQL™ Brain Tumor Module were summarized as mean, standard deviation, median, minimum and maximum scores, and percentages of floor (0) and ceiling (100) scores. The concordance between child- and parent-reports was determined using intraclass correlation coefficients (ICC) in the two-way mixed effects model [26].

Feasibility was determined based on the amount of time required to complete the pilot questionnaire and the percentage of missing values. Independence of easily missed items was tested by Cochran's Q test. Reliability was tested by internal consistency and retest reliability. Good internal consistency was defined as a Cronbach's coefficient alpha value exceeding 0.70. To determine retest reliability, the ICC between the initial test and retest scores in the one-way random effects model was examined, with an ICC value of 0.40 representing moderate, 0.60 good, and 0.80 high agreement.

Validity was tested by factorial validity, known-groups validity, and convergent and discriminant validity. Exploratory factor analyses using the principal factor method and the promax rotation were conducted on the 24 items. To describe known-groups validity, 95% confidence intervals between groups were calculated. We initially predicted that the Cognitive Problems scale scores would be low among children who had received whole brain irradiation and those with developmental impairment (mental retardation or learning disability), that the Movement and Balance scale scores would be low among children with infratentorial tumor and those with paresis, and that the Nausea scale score would be low among children currently undergoing chemotherapy.

Convergent and discriminant validity was examined by correlating the scales of the Japanese version of the PedsQL™ Brain Tumor Module with the theoretically-predicted scales of the PedsQL™ Generic Core Scales and STAIC. Pearson's product-moment correlation coefficient was calculated and corrected for attenuation [27]. We initially predicted that the Cognitive Problems scale would correlate relatively with the School Functioning scale, the Movement and Balance scale with the Physical Functioning scale, the Procedural Anxiety scale with the Emotional Functioning and the Trait Anxiety scales, and the Worry scale with the Emotional Functioning scale.

As our study was the first to give standard score distributions for the PedsQL™ Brain Tumor Module in Japan, we did not set ceilings on the sample size. Instead, we set a ceiling of four months on the study duration. Power analysis using the findings from the original English version [16] demonstrated that the minimum requisite sample size was 85 subjects, allowing for a specificity of 0.95 and a power of 0.8 for medium correlation (0.3) in the examination of convergent and discriminant validity. For the retest, the sample size was set at 22 subjects to achieve a specificity of 0.95 and a power of 0.8, allowing for observation of ICC values of 0.5 or greater for ICC parameters of 0.8 [28].

Ethical considerations

This study was approved by the review boards of all seven participating institutions. In consideration of the Japanese sociocultural environment, we avoided using the terms "cancer" or "tumor" with the children, using alternate terms in introductory writings and questionnaires. For participation of children aged 13 or over, informed consent from both children and parents was required. For participation of children aged 12 or under, informed assent from the child and informed consent from the parents was required.

Results

Sample characteristics

The median age of the children was 10.0 years (Table 1). The sample was heterogeneous with respect to tumor pathology and treatment experiences, and median time from diagnosis was 2.4 years. Sixty children (36.1%) had undergone whole brain irradiation at a median age of 7.0 years old, a median of 2.8 years before answering the questionnaire. Sixty parents (36.6%) regarded their own economic status and life as "affluent", in that they were financially secure and comfortable in their daily living.

Table 1: Subject Characteristics

	Number of respondents (n)	% of total	Median (years)	Range (years)
Age	166	100	10.0	2 - 18
Sex				
Male	91	55.2		
Female	74	44.8		
Tumor Pathology				
Embryonal tumors	47	29.0		
Germ cell tumors	36	22.2		
High-grade glioma	25	15.4		
Low-grade glioma	39	24.1		
Other	15	9.3		
Time from diagnosis	165	99.4	2.4	0.1 - 16.8
Period				
Inpatients	42	25.3		
Outpatients on treatment	23	13.9		
Outpatients with scheduled follow-up	99	59.6		
Outpatients without scheduled follow-up	2	1.2		
Medical history				
Cancer	3	1.8		
Heart disease	4	2.4		
Neurofibromatosis	2	1.2		
Treatment received				
None	5	3.0		
Surgery (S)	23	13.9		
Radiation (R)	1	0.6		
Chemotherapy (C)	4	2.4		
S+R	16	9.6		
S+C	24	14.5		
R+C	5	3.0		
S+R+C	88	53.0		
Have experience with stem cell transplantation				
Yes	17	10.2		
No	149	89.8		
Have experience with whole brain irradiation				
Yes	60	36.1		
No	106	63.9		

Table 1: Subject Characteristics (Continued)

Age at whole brain irradiation	60	36.1	7.0	0 - 18
Time since whole brain irradiation	60	36.1	2.8	0.0 - 14.8
Subjective opinion regarding own economic status and life				
Affluent	60	36.6		
Not affluent	104	63.4		
Relationship of parent to child				
Mother	153	92.2		
Father	10	6.0		
Grandmother	2	1.2		
Grandfather	1	0.6		
Academic background of parents				
Junior high school	3	1.8		
High school	64	39.3		
Vocational school	28	17.2		
Junior college	29	17.8		
University (undergraduate)	36	22.1		
University (graduate)	3	1.8		

Total (n) = 166
Missing data were excluded.

Scale descriptions

Values for all scales except the Pain and Hurt scale fell in the possible range of 0 to 100 (Table 2). For both child- and parent-reports, ranges of values for the Pain and Hurt scale were relatively narrow and placed higher. Over half of surveyed children (52.2%) reported the maximum score possible on the Movement and Balance Scale. Scale scores for all scales were consistently higher for the child-reports than for the parent-reports. Comparatively good concordance was seen between the child- and parent-reports for the Movement and Balance, Procedural Anxiety, and Nausea scales. In contrast, relatively poor concordance was seen between the two reports for the Worry scale.

Feasibility

With regard to time required to complete the pilot questionnaire, 4-11 minutes was required for completion of the child-report and 2-6 minutes for the parent-report, with 1.6% and 0.8% of values missing, respectively. The percentage of missing values for each item was independent (P = 0.84 for child-report, 1.00 for parent-report).

One child with mental retardation, diagnosed as 2-4 developmental years old, was unable to answer the child-report questionnaire, although his parent was able to answer the parent-report. One parent of a bedridden child unable to indicate his intentions could not answer the parent-report questionnaire.

Of the children at an eligible age to self-administer the questionnaire, 19 (17%) were interviewer-administered (1 with mental retardation, 2 with difficulty understanding the questionnaire, 1 with difficulty sustaining attention, 2 with difficulty reading, 7 with optical impairment, 2 with difficulty writing by hand, 2 with both optical impairment and difficulty writing by hand, and 2 experiencing fatigue). All 19 were able to answer the self-report under interviewer-administration.

Reliability

All scales except the Pain and Hurt scale for the child-report indicated good internal consistency (Cronbach's coefficient alpha = 0.50) (Table 3). On examination by age-appropriate format, good internal consistency was not observed in the Nausea scale for the young children (5-7 years old) child-report and in the Worry scale for